JOURNAL OF AIRCRAFT
Vol. 40, No. 2, March–April 2003

Probabilistic Two-Phase Wake Vortex Decay and Transport Model

Frank Holzäpfel*
DLR, German Aerospace Research Center, D-82234 Weßling, Germany

A new parametric wake vortex transport and decay model is proposed that predicts probabilistic wake vortex behavior as a function of aircraft and environmental parameters in real time. The probabilistic two-phase wake vortex decay model (P2P) accounts for the effects of wind, turbulence, stable stratification, and ground proximity. The model equations are derived from the analytical solution of the spatiotemporal circulation evolution of the decaying potential vortex and are adapted to wake vortex behavior as observed in large-eddy simulations. Vortex decay progresses in two phases, a diffusion phase followed by rapid decay. Vortex descent is a nonlinear function of vortex strength. Probabilistic components account for deviations from deterministic vortex behavior inherently caused by the stochastic nature of turbulence, vortex instabilities, and deformations, as well as uncertainties and fluctuations that arise from environmental and aircraft parameters. The output of P2P consists of confidence intervals for vortex position and strength. To assign a defined degree of probability to the predictions reliably, the model design allows for the continuous adjustment of decay parameters and uncertainty allowances, based on a growing amount of data. The application of a deterministic version of P2P to the Memphis wake vortex database yields favorable agreement with measurements.

Nomenclature

A	=	constant
b	=	vortex spacing
g	=	gravitational acceleration
N	=	Brunt–Väisälä frequency
q	=	rms turbulence velocity
R	=	mean radius
Ri	=	Richardson number
r	=	radial coordinate
r_c	=	core radius
T	=	parameter for vortex age
t	=	time
u	=	axial velocity
v	=	lateral velocity
w	=	descent speed
y	=	spanwise coordinate
z	=	vertical coordinate
Γ	=	circulation
Δt	=	time step
ε	=	eddy dissipation rate
Θ	=	potential temperature
ν	=	(effective) kinematic viscosity

Subscripts

l	=	lower limit
u	=	upper limit
0	=	initial value
1	=	first decay phase
2	=	second decay phase
5–15	=	average over circles with radii from 5 to 15 m

Superscripts

$*$	=	normalized quantity
$-$	=	mean quantity

Introduction

AS a consequence of lift, aircraft generate a pair of long-lived counter-rotating wake vortices that bear a potential risk for following aircraft. Current wake-vortex separation standards between consecutive aircraft contribute significantly to the capacity constraints of congested airports. From experience and research results gained during the past 30 years, it has become evident that the separation standards may be overly conservative for a variety of meteorological situations.[1,2] A parametric model capable of reliably predicting vortex positions and strengths in real time in a measured or forecasted atmospheric environment along the glide path might, therefore, permit air-traffic controllers to ease some of the regulations without loss of safety. Several reduced spacing systems[3–5] that employ vortex decay and transport models of different complexity have been developed. However, none of the systems is operational today. Other applications of parametric wake vortex models include encounter investigations within flight simulation environments, for example, Ref. 6, safety analyses that estimate the hazard probability of new approach and landing procedures,[7] and studies that simulate different aspects of reduced spacing systems, for example, the predictability of wake vortices based on virtual environmental measurement data in a convectively driven atmospheric boundary layer.[8]

The first wake vortex model presented in 1986 by Greene[9] assumes that the impulse per unit length of a wake is reduced by the sum of viscous drag, buoyancy force, and turbulent decay. From a single equation, circulation, velocity, and vertical position of the wake can be determined. Greene's model was extended by Corjon and Poinsot[10] by adding ground and crosswind effects 10 years later. Sarpkaya[11] eliminated the viscous drag in Greene's[9] model and proposed an empirical model for turbulent decay that relies on the eddy dissipation rate instead of turbulent kinetic energy. More recently, Sarpkaya et al. adapted the descent rate to observations by introducing variable vortex spacing.[12] The Canadian vortex forecast system[13] models the evolution of multiple discrete vortices in a two-dimensional crossplane starting from a near wake database that acounts for the aircraft geometry. Effects of the ground and nonuniform wind shear are included; decay due to ambient turbulence is

Received 30 November 2001; revision received 8 October 2002; accepted for publication 12 October 2002.

*Research Scientist, Institute of Atmospheric Physics, Oberpfaffenhofen.

adapted from approaches from either Ref. 9 or 11. Another model that accounts for effects of ambient turbulence, crosswind shear, and ground proximity was proposed by Kantha.[14] Recently, Mokry[15] presented a two-dimensional continuous vortex sheet method that captures vortex sheet rollup, interaction with ambient shear layers and the ground.

Note that despite the significant number of available wake vortex models none of these models considers all effects of the first-order impact parameters, which are aircraft configuration, turbulence, stable stratification, shear, and proximity of the ground. In particular, they are all deterministic. Not specified are deviations from predicted values that are inherently caused by the stochastic nature of turbulence, complex vortex instabilities and deformations, uncertainty of aircraft parameters, and uncertainties and fluctuations of environmental parameters. The probabilistic two-phase wake vortex decay model (P2P) proposed here is designed to predict wake vortex behavior within defined confidence intervals. For this purpose, the model concept allows for the continuous adjustment of decay parameters and uncertainty allowances, based on a growing amount of observations and simulations. Currently, the decay parameters are "calibrated" based on different large-eddy simulation (LES) data.[16,17] The LES data suggest that vortex decay progresses in two phases, a diffusion phase followed by rapid decay,[1,18] and that vortex descent is not a linear function of vortex strength. The model accounts for the effects of wind, turbulence, stable stratification, and ground proximity. Wake shear-layer interaction is not parameterized. It is believed that the associated complex vortex behavior[19] cannot be predicted reliably in an operational environment. Situations where shear layer effects are not covered by uncertainty allowances have to be diagnosed, and reduced spacing operations must be ruled out.

After an introduction of the model concept, the equations that describe circulation decay and descent rate are derived and adapted to the LES data. Then the probabilistic components of P2P are discussed. The paper concludes with applications of P2P to the Memphis wake vortex database.[20] A comprehensive comparison to different measurements[20,33,34] is in preparation.

Model Concept

P2P is designed to include as much knowledge as possible gained from both experimental and numerical wake vortex research with a focus on operational needs. For this purpose the model concept comprises the following elements.

First, in contrast to most other models, P2P employs a well-defined and experimentally accessible definition for vortex strength. Unlike single vortices where the circulation reaches a definite constant value at large radii, the circulation of vortex pairs strongly depends on the method of its evaluation. P2P uses a circulation Γ_{5-15} that is averaged over circles with radii from 5 to 15 m or, alternatively, from 3 to 10 m, for several reasons. 1) The estimation of the root circulation may be extremly difficult for a vortex pair that evolves in the atmosphere. This is the case in measurement and simulation. At radii where $\Gamma(r)$ should run into saturation, influences of the neighbouring vortex, secondary vortices, ambient turbulence, or baroclinic vorticity may drastically modify the circulation values. The upper integration limit of $r = 15$ m avoids these difficulties for larger aircraft. 2) The averaging of Γ over a radius interval reduces the scatter in turbulent vortices and enables estimations of disintegrating vortices. 3) Small radii that are not reliably accessible by lidar are excluded. 4) Because the final aim of P2P is to predict vortex behavior to allow for dynamic spacing between consecutive aircraft, an operationally useful circulation definition is employed that correlates well with effects of potential wake encounters.[21] Note that Γ_{5-15} is only calculated from the velocity components that are perpendicular to the flight direction or from the corresponding vorticity, regardless of the actual orientation of the vortex axis. This implies that large-scale deformations or the formation of the Crow instability may considerably reduce Γ_{5-15}, whereas circulation in a local plane perpendicular to the vortex axis is not necessarily mitigated.

Second, P2P is based on a well-founded equation for vortex evolution. Because there is no rigorous solution for the evolution of turbulent vortex pairs, the hydrodynamic basis of P2P relies on the equation that describes the spatiotemporal circulation evolution of the decaying potential vortex

$$\Gamma(r,t)/\Gamma_0 = 1 - \exp(-r^2/4\nu t) \tag{1}$$

Equation (1) constitutes an analytical solution of the Navier–Stokes equations for a non-stationary, plane, rotating flow.[22] In P2P, this relation is extended and adapted to LES results of different groups[16,17] to describe vortex decay and descent.

Third, P2P contains probabilistic components to meet the variability of wake vortex behavior that is caused by manifold governing physical mechanisms,[23] turbulence, and uncertainties regarding environmental conditions. The output of P2P consists of lower and upper bounds for vortex position and circulation. The final goal is to determine reliably the probability with which the actual vortex evolution is met by predictions. For this purpose, P2P has to be applied to as much available data as possible to give it an outmost broad phenomenological and statistical basis. The design of P2P allows an ongoing adaption to observations and an adjustment to a desired confidence level.

The model is formulated in normalized form where the characteristic scales are based on initial vortex separation and circulation leading to the timescale

$$t' = 2\pi {b_0}^2 \big/ \Gamma_0 = b_0/w_0 \tag{2}$$

Circulation

It is assumed that the evolution of Γ^*_{5-15} can be described by two consecutive decay phases as observed in LES[16,17] (Figs. 1 and 2). In the first phase, termed diffusion phase, the normalized, radii-averaged circulation can be formally calculated as

$$\Gamma^*_{5-15}(t^*) = \frac{1}{11}\sum_{r=5\,\mathrm{m}}^{15\,\mathrm{m}} A - \exp\frac{-r^{*2}}{4\nu_1^*\left(t^* - T_1^*\right)} \tag{3}$$

Because the vortices are not decaying potential vortices but are generated by the rollup of a vorticity sheet, an adaption of vortex parameters is introduced by the constants A and T_1^* where $-T_1^*$ corresponds to the age of the vortices at $t^* = 0$ and reflects the vortex structure at that time. A is a constant to adjust $\Gamma^*_{5-15}(t^* = 0)$. Figure 3 shows a comparison of Eq. (3) with $A = 1.09$, $T_1^* = -2.22$, and an effective viscosity $\nu_1^* = 1.78 \times 10^{-3}$ ($\nu_1 = 0.16$ m^2/s) to the LES baseline case[16] of a vortex evolution in a quiescent, neutrally stratified atmosphere.

For the sake of simplicity, the averaging over different radii as performed in Eq. (3) is omitted, which leads to

$$\Gamma^*_{5-15}(t^*) = A - \exp\left[-R^{*2}\big/\nu_1^*\left(t^* - T_1^*\right)\right] \tag{4}$$

The mean radius R^* corresponds approximately to the mean value of 10 m within the averaging interval 5–15 m. R^{*2}, which includes the

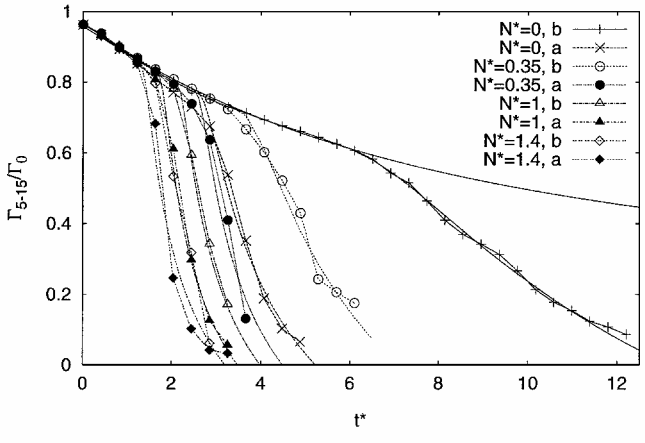

Fig. 1 Circulation from LES[16] and respective fits of P2P for different turbulence scenarios and different degrees of stratification.

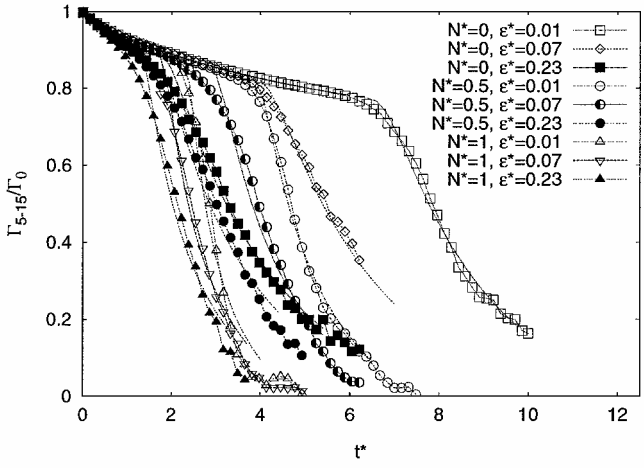

Fig. 2 Circulation from LES[17] and respective fits of P2P for different degrees of turbulence and stratification.

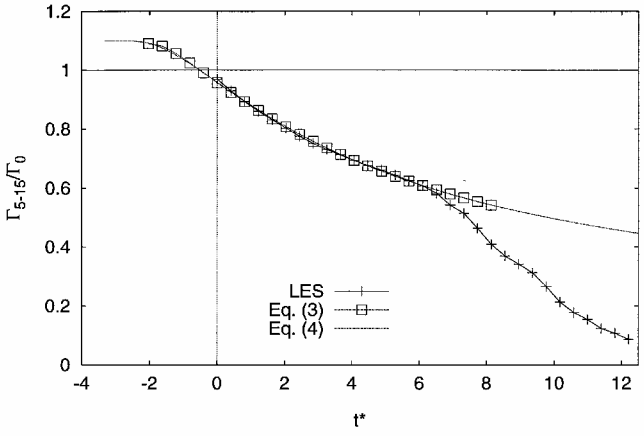

Fig. 3 Circulation evolution in the diffusion phase for LES[16] in quiescent atmosphere and respective fits with Eqs. (3) and (4).

factor one-quarter of Eq. (3), is determined as 0.0121. (In the LES, $b_0 = 47$ m.) The parameters $A = 1.1$ and $T_1^* = -3.48$ are slightly modified, whereas the viscosity remains unchanged. This simplification still gives a very good representation of the diffusion phase (Fig. 3).

The second phase is called the rapid decay phase. Different instability and decay mechanisms,[19,24] as well as large-scale deformations (deviation of local vortex axis from flight direction), lead to an accelerated reduction of Γ^*_{5-15}. The original cause for the release of the rapid decay phase (turbulence, stable stratification, shear) may be diverse, and also many details of the respective mechanisms may vary considerably from case to case. Nevertheless, it is assumed that in all cases a two-phase evolution of Γ^*_{5-15} prevails as observed in numerical investigations[16,17,25] and lidar measurements.[26] The rapid decay phase is described by

$$\Gamma^*_{5-15}(t^*) = A - \exp\left[-R^{*2}\Big/\nu_1^*\left(t^* - T_1^*\right)\right] - \exp\left[-R^{*2}\Big/\nu_2^*\left(t^* - T_2^*\right)\right] \tag{5}$$

where the onset time of rapid decay at T_2^* and the respective decay rate that is adjusted by the effective viscosity ν_2^* depend on meteorological parameters. Figures 1 and 2 show circulation evolutions from our LES[16] and from the LES of Proctor and Switzer[17] together with the respective fits of P2P for different turbulence levels and different degrees of stable temperature stratification. Stratification is characterized with a normalized Brunt–Väisälä frequency [discussed later in Eq. (16)]. Our LES distinguish between two cases case b, where only aircraft-induced turbulence is superimposed on the vortices, and case a, where the turbulent vortices evolve in an anisotropic atmospheric turbulence with rms velocities of 0.38 m/s in the horizontal and 0.21 m/s in the vertical directions, respectively. Proctor and Switzer characterize turbulence with the normalized eddy dissipation rate, $\varepsilon^* = (\varepsilon b_0)^{1/3}/w_0$. The LES of both Refs. 16 and 17 show that the initial decay rate is very similar for the different cases. The reduced decay rate observed in the diffusion phase of Proctor and Switzer's[17] LES is mainly caused by their Richardson number correction for rotational effects (see Ref. 27), which reduces the diffusion in the vortex core region. The higher the turbulence and the stronger the stratification, the earlier the individual curves detach from their common evolution in the diffusion phase to initiate the rapid decay phase. The effect of aircraft-induced turbulence (case b) seems to correspond roughly to the effect of ambient turbulence with an eddy dissipation rate of $\varepsilon^* = 0.01$. The good agreement of the fits of P2P according to Eqs. (4) and (5) with the LES substantiates the appropriateness of the approach.

Decay Parameters

The values of T_2^* and ν_2^* have to be determined as functions of meteorological parameters. Basically, the impact of turbulence can be parameterized based on turbulent kinetic energy (TKE) or, alternatively, eddy dissipation rate. An analysis[28] of 525 wake vortex measurements of the Memphis database evaluates the potential of the respective quantities. Figure 4 shows cumulative distributions of the instant in time of the last circulation measurement by lidar for three different turbulence regimes. It is assumed that this instant in time is correlated to the longevity of the vortices. The TKE* criterion shown in Fig. 4a separates vortex longevity in the low- and intermediate turbulence regimes insufficiently, whereas the correlation

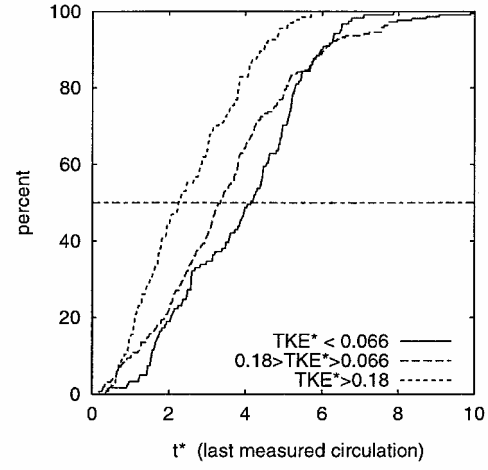

a)

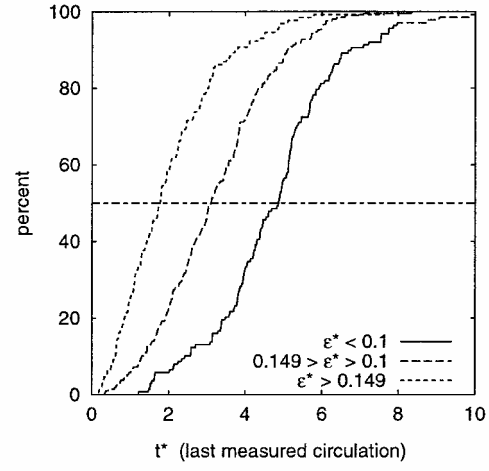

b)

Fig. 4 Cumulative distribution of the time of last lidar measurement of 525 cases for three different classes of turbulence characterized by a) normalized TKE and b) normalized eddy dissipation rate.

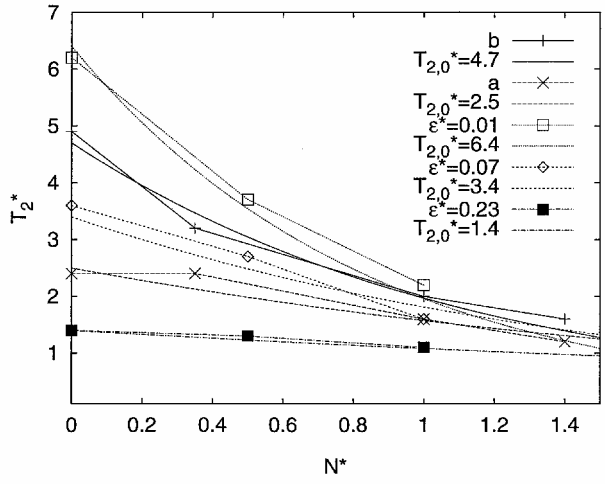

Fig. 5 Decay parameter, T_2^*, as a function of stratification and turbulence determined for LES (symbols) and corresponding fits to Eq. (6).

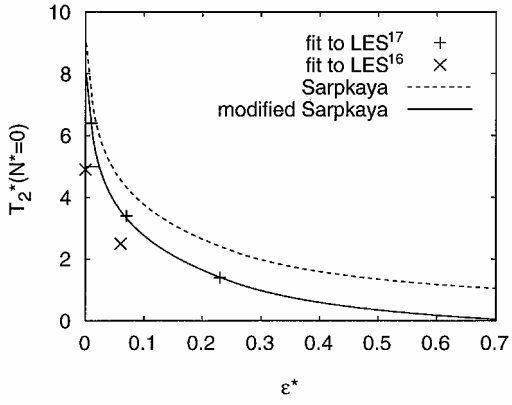

Fig. 6 Decay parameter T_2^* for neutral stratification as a function of ε^* for different LES, the Sarpkaya[11] model and a modification of Sarpkaya's model.

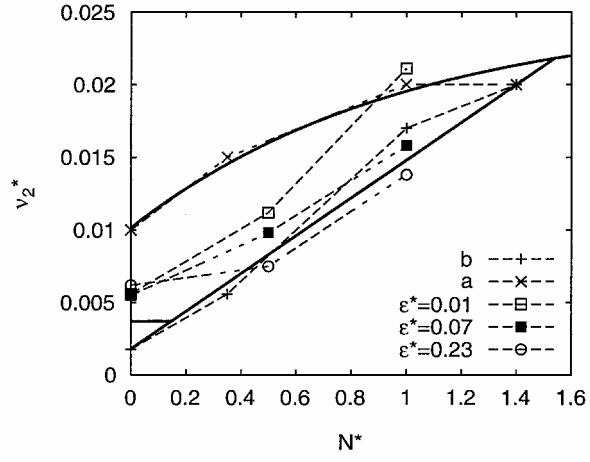

Fig. 7 Decay parameter ν_2^* as function of stratification for different turbulence levels as fitted to LES[16,17] and corresponding limiting curves (——) according to Eqs. (9) and (10).

of longevity and ε^* shown in Fig. 4b is much more distinct. This result corroborates the assumption[11] that the intensity of atmospheric fluctuations in the length-scale range that affects vortex decay may be well characterized by ε^*, that is, the crucial length-scale range of wake vortices resides in the inertial subrange of turbulence spectra of atmospheric boundary layers. In contrast, TKE* data are sensitive to the choice of the averaging time frame, that is, the longer the averaging interval, the more energy is contributed from larger scales that are irrelevant for vortex decay. Therefore, in P2P, the parameterization of the impact of turbulence is based on ε^*, although it is difficult to deduce ε^* from measurements in an operational environment.

Figure 5 shows the dependency of T_2^* [determined by fitting Eq. (5) to the LES data] on N^* for different turbulence levels. Increased values of turbulence and stratification both reduce T_2^*. As soon as turbulence or stratification is strong, the impact of the other respective parameter becomes minor. Note that the onset time of rapid decay, T_2^*, coincides well with visually determined inflexion points of the Γ_{5-15}^* curves (Figs. 1 and 2) and, remarkably, also with the point in time at which axial cross sections of vorticity show a transition[19] from a quasi-laminar state (turbulence on length scales $L \ll r_c$) to a fully turbulent state [$L = \mathcal{O}(r_c)$]. Both transition and inflexion point concurrently indicate that the flow state enters the rapid decay phase. The family of curves in Fig. 5 that correspond to specific turbulence levels can be fitted by

$$T_2^* = T_{2,0}^* \exp\left(-0.185 T_{2,0}^* N^*\right) \tag{6}$$

where the turbulence level is characterized by the time constant for rapid decay in the neutrally stratified atmosphere, $T_{2,0}^* = T_2^*(N^* = 0)$.

The dependency of $T_{2,0}^*$ on ε^* for the LES data is shown in Fig. 6 by symbols. Furthermore, the model of Sarpkaya[11] that relates the time at which a "catastrophic demise event" takes place in nonstratified environments to ε^* is displayed. The Sarpkaya[11] approximation is based on various analyses, observations, and simulations and covers a wide range of turbulence intensities. Subtracting one timescale from the Sarpkaya[11] curve (modified Sarpkaya) yields very good agreement with the data derived from Proctor and Switzer's[17] LES. P2P takes advantage of the extrapolation of Proctor and Switzer's data to higher turbulence levels by the Sarpkaya[11] model for $\varepsilon^* > 0.0235$,

$$T^* = 0.804 \varepsilon^{*\frac{3}{4}}, \qquad \varepsilon^* > 0.2535$$

$$T^{*\frac{1}{4}} \exp(-0.70 T^*) = \varepsilon^*, \qquad \varepsilon^* > 0.0235 \tag{7}$$

and adapts it according to $T_{2,0}^* = T^* - 1$ (Fig. 6, solid line). For $\varepsilon^* \leq 0.0235$, our conservative baseline LES case in which wake vortices are initialized with superimposed aircraft-induced turbulence in a quiescent, neutrally stratified atmosphere provides the upper threshold

$$T_{2,0}^* = 5, \qquad \varepsilon^* \leq 0.0235 \tag{8}$$

The T_2^* values that are calculated from Eqs. (6–8) are varied by $\pm 20\%$ in two subsequent runs of P2P to account for uncertainties of T_2^*.

Figure 7 shows that the correlation of ν_2^* values with turbulence and stratification is less distinct than for T_2^*. The LES of Proctor and Switzer[17] and our LES even give contrary tendencies: In our LES, the strongest impact of turbulence is found for neutral stratification, whereas Proctor and Switzer's nonstratified data are insensitive to turbulence. Moreover, in a stably stratified atmosphere, the two LES approaches yield opposite trends regarding the dependency of ν_2^* on turbulence. Therefore, ν_2^* is parameterized only as a function of N^*, and the uncertainty of the impact of turbulence is taken into account by performing two consecutive P2P-runs that employ the upper and lower bounds of ν_2^* for a given value of N^*. The upper boundary follows

$$\nu_{2,u}^* = 0.025[1 - \exp(-N^* - 0.52)] \tag{9}$$

and the lower boundary is given by

$$\nu_{2,l}^* = 0.0018 + 0.013 N^* \tag{10}$$

Furthermore, a threshold of $\nu_{2,l}^* = 0.0037$ is introduced when $\varepsilon^* > 0.01$ to avoid extensively long-lived vortices in a weakly turbulent environment. Values below that threshold are only applied for essentially quiescent ambient flows.

There is no height variation of meteorological impact parameters in the LES data used for calibration. If measurements or predictions of vertical profiles of $\varepsilon^*(z^*)$ and $N^*(z^*)$ are available, P2P employs a running average. The running average allows a weighting of the impact of the environmental conditions according to the respective residence time of the vortices at a particular vertical position. For example, the running average of the eddy dissipation rate is calculated according to

$$\bar{\varepsilon}^*(t^*) = [(t^* - \Delta t^*)\bar{\varepsilon}^*(t^* - \Delta t^*) + \Delta t^* \varepsilon^*(t^*)]/t^* \tag{11}$$

where the running average is updated every time step. If local wind data are available, the vortices are transported by all available wind components including vertical wind.

Descent Speed

The simple relation $w^* = \Gamma^*$ holds only if Γ^* represents the circulation at the neighboring vortex. For radii-averaged circulations such as Γ^*_{5-15}, it is not valid. LES and observations indicate that Γ^*_{5-15} may decrease substantially without considerable influence on the descent speed.[16] This can readily be understood by considering the simple decaying potential vortex whose tangential velocities decrease less at radii that induce the descent speed for larger aircraft ($b > 15$ m) than in the radii interval $5 \le r \le 15$ m that is used for determination of Γ^*_{5-15}. However, wake vortices do not evolve like single laminar vortices. Nevertheless, the strategy to develop a relation between w^* and Γ^*_{5-15} again is to employ the laminar decaying potential vortex as a basis that is adapted to the behavior observed in LES.

Given the assumption that the vortices decay in accordance with the self-similar velocity profiles of the potential vortex, the descent speed can be calculated as a function of vortex spacing and core radius according to

$$w^* = 1 - \exp\left(-1.257 b^2 / r_c^2\right) \tag{12}$$

The relation between descent speed and Γ^*_{5-15} is then implicitly given via the core radius by

$$\Gamma^*_{5-15} = \frac{1}{11} \sum_{r=5\,\mathrm{m}}^{15\,\mathrm{m}} 1 - \exp \frac{-1.257 r^2}{r_c^2} \tag{13}$$

Figure 8 illustrates Eq. (13) graphically. Figure 9 shows the relation of Γ^*_{5-15} and descent speed for different vortex separations given by Eqs. (12) and (13). Note that this relation is an implicit function of core radius. For aircraft that already have small vortex separations, a slight decrease of Γ^*_{5-15} (caused by an increase of core radius) would decrease the descent speed, whereas for large vortex separations, the descent speed would be affected only when Γ^*_{5-15} reaches small values, that is, when the core radius is of the order of vortex separation. Comparison with the descent speed observed in the LES baseline case (Fig. 9) indicates that Eqs. (12) and (13) yield a

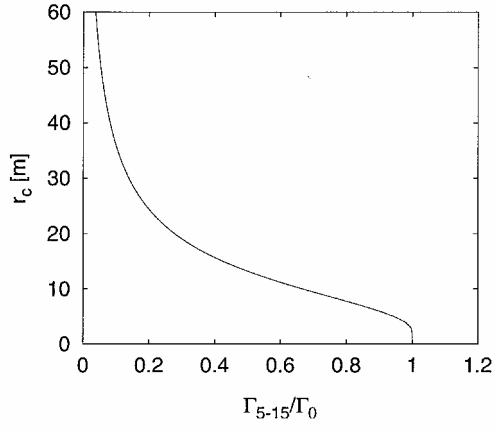

Fig. 8 Relation of r_c and Γ^*_{5-15} for decaying potential vortex.

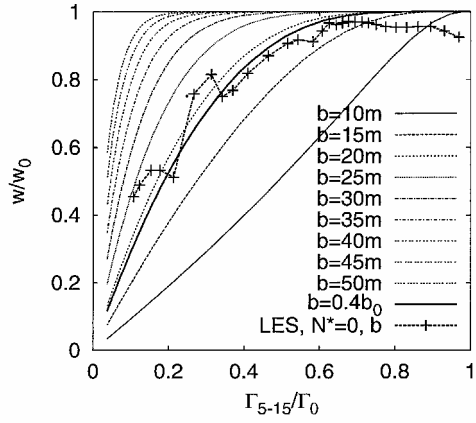

Fig. 9 Relation of descent speed and Γ^*_{5-15} for different vortex separations and LES baseline case,[16] $b_0 = 47$ m.

useful approximation with an effective vortex spacing of $b = 0.4b_0$. To avoid an iterative solution of Eq. (13) during model predictions, the effective core radii r_c are interpolated as a function of Γ^*_{5-15} using a look-up table.

In stably stratified cases, the buoyancy force additionally reduces the descent speed. This effect is not contained in the kinematic approximation given by Eqs. (12) and (13). Therefore, Greene's slightly modified concept of impulse reduction by the buoyancy force[9] is calculated in parallel to the earlier described algorithm to yield a descent speed $w^*_{\mathrm{buoy}} = \Gamma^*_{\mathrm{buoy}}$, where Γ^*_{buoy} results from

$$\frac{\mathrm{d}\Gamma^*_{\mathrm{buoy}}}{\mathrm{d}t^*} = 0.4525 N^{*\sqrt{2}\cdot 2} \Delta z^* \tag{14}$$

The resulting descent speed is then obtained by weighting w^* [from Eq. (12)] with the relative decrease of the descent speed due to buoyancy, $w^*_{\mathrm{buoy}}/w^*_0 = w^*_{\mathrm{buoy}}$, according to

$$w^*_{\mathrm{res}} = w^* w^*_{\mathrm{buoy}} \tag{15}$$

Model results with LES[16] show that the descent speed is underestimated for $N^* < 1$ and overestimated for $N^* > 1$. This is due to a decrease of vortex separation for $N^* < 1$ and an increase of vortex separation for $N^* > 1$. The superscript $\sqrt{2}$ used in Eq. (14) for N^* yields a good correction for the vortex-spacing modified descent speed. The normalized local Brunt–Väisälä frequency is defined as

$$N^* = [g/\Theta_0(\Delta\Theta/\Delta z)]^{\frac{1}{2}} t' \tag{16}$$

The nonlinear dependency of descent rate on circulation gives P2P the following capabilities. 1) It allows for a reduction of circulation without the reduction of the descent rate during the early vortex evolution. Robins et al.[29] show in their case studies that the early trajectories, until the vortices leave a predefined corridor, are best predicted when the descent rate is not reduced by turbulent circulation decay, that is, the descent rate almost retains its theoretical value. 2) It allows for stagnating vortices with nonzero circulation in strongly stably stratified environments. In other models,[9,10] circulation and descent are coupled directly such that both quantities become zero at identical times. 3) It enables rebounding vortices in very strongly stratified environments. Rebound of vortices that is of high relevance for the safety of following aircraft occurs when $w^*_{\mathrm{buoy}}/w^*_0$ becomes negative. All of these features are in accordance with LES data (Fig 10).

The effect of the ground on vortex trajectories is modeled following the approach of Robins et al.[29]. Image vortices are introduced when the primary vortices have reached a height of $1.5b_0$ above ground. At a height of $0.6b_0$, counter-rotating ground effect vortices and their respective image vortices are introduced at an angle of 45 deg inboard below the primary vortices at a distance of $0.4b_0$. Another pair of secondary vortices with images is introduced when the first pair has rotated 180 deg around the primary vortices. The strength of the secondary vortices is a function of the rotation angle

and reaches a maximum of $\Gamma_s^* = 0.4w^*$ after traveling 90 deg. The decay rate is not modified in ground effect because a comparison of different decay models yields only negligible impact on vortex trajectories.

Probabilistic Approach

Precise deterministic wake vortex predictions are not feasible operationally for several reasons. Primarily, it is the nature of turbulence that deforms and transports the vortices in a stochastic way and leads to considerable spatiotemporal variations of vortex position and strength. Moreover, aircraft parameters, and especially the state of the atmospheric boundary layer with its intrinsic variability, can only be measured or predicted with limited accuracy. Finally, uncertainties with respect to the accuracy of circulation and position derived from lidar measurements add up in a comparison of measurement and prediction. The scatter resulting from all of these factors only allows the prediction of wake vortex behavior within uncertainty bounds and a respective probability.

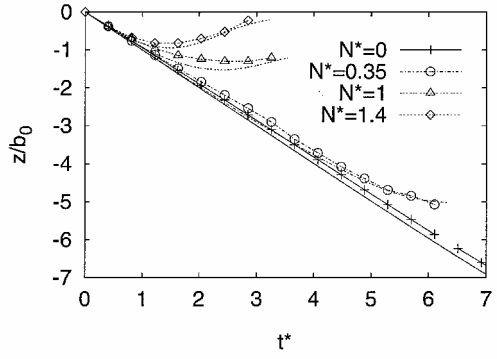

Fig. 10 Comparison of descent between LES[16] (symbols) and P2P (lines) in quiescent atmosphere with different degrees of stratification.

P2P uses several components that take into account these uncertainties. Figure 11 shows exemplarily the output of P2P that consists of upper and lower bounds for vertical and lateral position, as well as circulation. Two runs, each with a combination of decay parameters for the upper bound ($T_{2,u}^* = 1.2\,T_2^*$, $\nu_{2,u}^*$) and lower bound ($T_{2,l}^* = 0.8\,T_2^*$, $\nu_{2,l}^*$), vary the onset time of rapid decay and the respective decay rate. For the diffusion phase, no parameter variations are performed because the early wake vortex evolution has no impact on aircraft separations. A constant uncertainty allowance of $0.2\,\Gamma_0^*$ is added to (subtracted from) the upper (lower) curve of circulation evolution. Obviously, only the upper limit of the circulation prediction is of practical significance because operational wake vortex predictions have to be conservative. For vertical and lateral position, an uncertainty allowance of one initial vortex spacing is employed. Additionally, the increased scatter of vortices in turbulent environments is modeled by the assumption that the rms value of ambient turbulence serve as superimposed propagation velocity. When started from the upper (lower) curves for descent rate and lateral displacement that result from decay parameter variations, the final upper (lower) bounding curves for vortex positions are calculated according to

$$y_{u(l)}^*, z_{u(l)}^* = y^*, z^* + (-)\left(1 + \int q^*(z^*)\,\mathrm{d}t^*\right) \qquad (17)$$

The validity of this approach was recently demonstrated for a convective boundary-layer situation.[8] In Fig. 11, the limiting curves

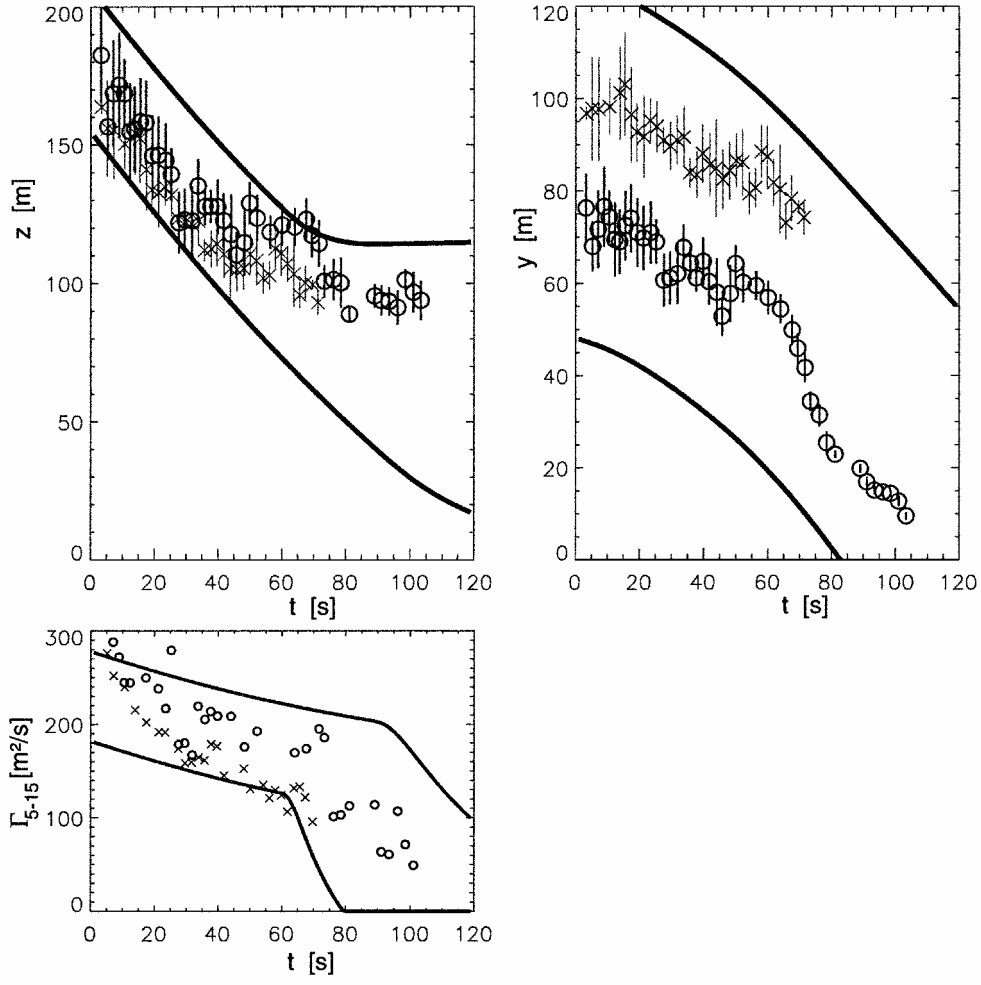

Fig. 11 Comparison of P2P predictions with lidar observations with error bars, for Memphis[20] case 1282 (B727 aircraft): ——, bounds of expected behavior; ○, port vortex: and ×, starboard vortex.

enclose almost all measured data. Only some operationally insignificant early circulation values are underestimated. Possibly the early circulation values that considerably exceed the theoretical circulation can be attributed to the rollup process of multiple vortices because the evaluation of lidar spectra, based on the assumption of axisymmetric vortices, employs the product of maximum velocity and distance to the vortex center. As a result, secondary vortices are interpreted as high tangential velocities on large radii, hence, high circulation.

Application

P2P essentially is designed to predict the bounds of wake vortex behavior in a probabilistic sense. The respective capabilities of P2P will be discussed in detail in another publication. Here, a deterministic version of P2P, where the uncertainty allowances are neglected, is applied to a larger number of Memphis wake vortex measurements.[20]

Obviously, the scatter of individual Memphis circulation data is too large to infer the typical decay characteristics of wake vortices. In particular, lidar measurements often cease at a level of circulation at which the rapid decay would set in, according to LES. A possible explanation is that the associated large-scale deformation and the transition to fully turbulent vortices complicate the evaluation of circulation. Moreover, highly precise lidar measurements in the late (second) phase of complex vortex evolution would render only a little representative data because they represent just a single plane. Only the averaging along many planes would yield meaningful Γ^*_{5-15} values.

Therefore, in this section, a statistical approach is followed in which a large number of cases that meet specific criteria[28] are averaged. The resulting mean behavior is discussed to evaluate basic capabilities and properties of the model formulation, in particular, with respect to the two-phase circulation decay. Environmental conditions are classified according to wake vortex behavior classes[30] that are based on a bulk Richardson number[31]

$$Ri_b = N^2 \Big/ \left(\frac{\Delta u}{\Delta z}\right)^2 + \left(\frac{\Delta v}{\Delta z}\right)^2 \tag{18}$$

where the vertical gradients of the mean horizontal wind components are considered in a height interval that ranges from 40 to 200 m. There are 144 cases assigned to the class stable stratification defined by $Ri > 1$ and 138 cases to the class turbulence with $Ri < 0.25$. The eddy dissipation rate is calculated from spectra that are established from 30-min averages of ultrasonic anemometer measurements on a 40-m-high tower. An average Brunt–Väisälä frequency is determined from measurements of potential temperature by soundings of a radio acoustic sounding system and radio sondes. To avoid ground effects, only data of aircraft with a flight altitude above $5b_0$ is used. The initial height of the vortices is taken from beacon altitude.

The deterministic version of P2P applies two sets of decay parameters, T_2^* and ν_2^*, for a given environmental situation. To achieve an appropriate statistical weighting of the resulting predictions, these are varied in 11 consecutive runs in increments of 10% between their upper and lower bounds. The statistics of measurements, on the other hand, are susceptible to the duration of individual measurements and the resulting data mix. To ensure the comparability of measurement and prediction, the predictions are teminated when the magnitude of the last circulation measurement is reached or when the last vertical position is measured, respectively. Without this procedure, which provides an identical data mix in measurement and prediction, the resulting curves deviate substantially. Furthermore, the results are compared to Greene's[9] model that employs measurements of TKE

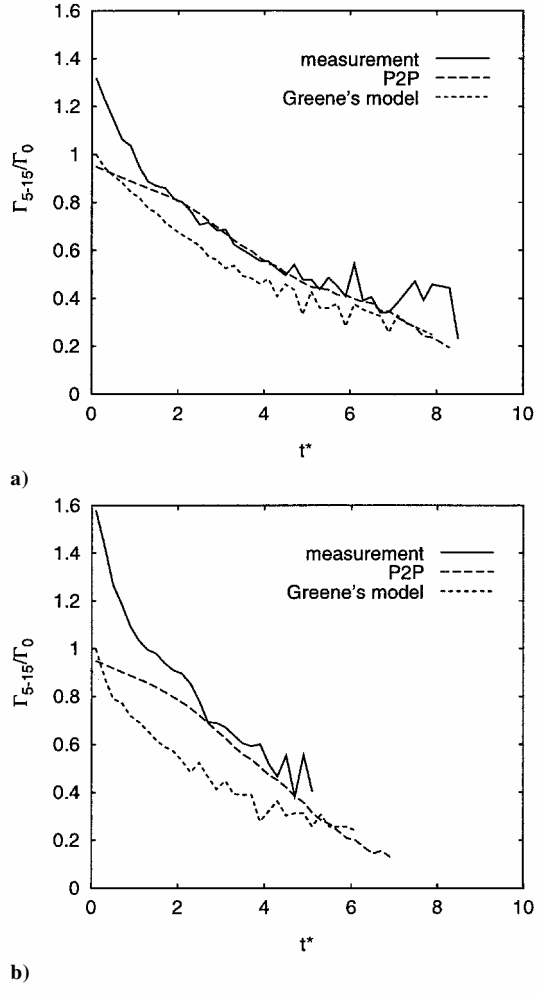

Fig. 12 Comparison of measured and predicted mean evolution of Γ^*_{5-15} in a) stable class (144 cases) and b) turbulent class (138 cases).

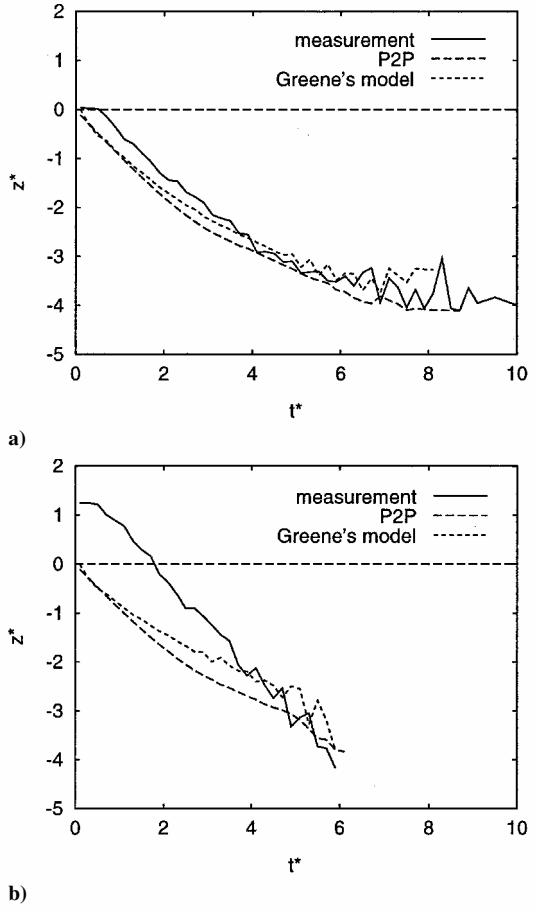

Fig. 13 Comparison of measured and predicted mean descent in a) stable class and b) turbulent class.

on the 40-m tower. The constant for turbulent decay is set to 0.41, according to Ref. 32.

Figure 12a demonstates very good agreement between measurements and P2P in the stable class when the initial overestimation of circulation by lidar is neglected. In the turbulent class (Fig. 12b) the overestimation of circulation is even more pronounced and persists longer so that agreement is achieved later. Note that the two-phase decay of P2P is masked completely in the mean evolution of Γ^*_{5-15}. This implies that the two-phase decay may well be hidden in the scatter of the lidar data (cf. Fig. 11). Greene's[9] model underestimates consistently and nonconservatively the circulation measurements. The measured vertical position shown in Fig. 13a indicates a delayed onset of descent that might reflect the rollup phase of the vortices. Such a delay could easily be implemented in P2P. Later, the descent rate is well predicted by P2P and slightly underestimated by Greene's model. In the turbulent case, the initial height is strongly overestimated for unknown reasons ($z^* = 0$ corresponds to beacon altitude), which makes it difficult to compare descent rates. Currently, P2P is applied to further data sets.[20,33,34]

Conclusions

A probabilistic real-time wake vortex transport and decay model termed P2P is proposed. Circulation decay and descent rate are parameterized in analogy to the decaying potential vortex. Detailed wake vortex characteristics achieved by high-resolution numerical simulations are transferred to the real-time model by the adjustment of parameters. The deviations between different LES determine the variability of the decay parameters. Circulation decay precedes in two phases, a gradual and a subsequent rapid decay. The respective decay rates are adjusted by an effective viscosity. The introduction of an effective vortex spacing and effective core radii allow the derivation of equations that describe the nonlinear dependence of descent rate and radii-averaged circulation and that reproduce descent characteristics found in LES and measurements. The favorable comparison of a deterministic version of P2P to measurement data has demonstrated the suitability of the two-phase approach. In particular, it is shown that the two-phase decay characteristics are hidden in the mean evolution of averaged measurement data. P2P accounts for all relevant environmental parameters, such as wind, turbulence, stable stratification, and ground proximity, with the exception of shear. It is assumed that the effects of constant background shear are well covered by the probabilistic approach. Because of the high sensitivity of wake vortex behavior on shear layer characteristics, it is believed that the associated complex vortex behavior cannot be predicted reliably in an operational environment. Situations where shear layer effects are not covered by uncertainty allowances have to be diagnosed, and reduced spacing operations must be ruled out.

Although good results have already been achieved without further adjustment of the model, the benefits of P2P will fully appear when a fine-tuning process has been accomplished based on a sufficiently large amount of data. Currently, P2P is applied to different data sets accomplished at Memphis International Airport,[20] Dallas-Fort Worth International Airport, the Aircraft Wake Vortex Prediction and Measurement Campaigns WakeOP at Fairchild-Dornier Airport, Oberpfaffenhofen, Germany, and WakeTOUL at Tarbes Airport, France. However, the quality of measurements used for tuning will affect the magnitude of uncertainty allowances. For example, the distance of the wind measurement site to the considered section of the glide path and the degree of homogeneity of the wind field will have a strong impact on the allowances for vortex dispersion. To achieve maximum accuracy and, consequently, maximum safety and efficiency of a reduced spacing system, a refined tuning process should be conducted for every individual site with its individual peculiarities. Another criterion for maximum operating efficiency is that the probabilities of the predicted confidence intervals should ideally be identical for all operationally relevant phases of vortex evolution. Therefore, a variable formulation of the currently static uncertainty allowances may be useful. Further refinements of P2P could be achieved by applying boundary-layer scaling laws to derive an anisotropic, height-dependent parameterization of turbulence-driven spreading of the confidence intervals. The scaling laws could be based on the diagnosed type of atmospheric boundary layer.

Acknowledgments

Thanks are extended to many friends and colleagues, such as Alexandre Corjon, Michael Frech, Thomas Gerz, and George Greene, who supported the current work by fruitful discussions and cooperation. In particular, Tobias Zinner for the Memphis data analysis, Fred Proctor and George Switzer for providing the large-eddy simulation data, and Robert Robins and Donald Delisi for their hospitality, support, and the ground effect model are acknowledged. The supply of the Memphis database by NASA Langley Research Center is greatly acknowledged.

References

[1]Gerz, T., Holzäpfel, F., and Darracq, D., "Commercial Aircraft Wake Vortices," *Progress in Aerospace Sciences*, Vol. 38, No. 3, 2002, pp. 181–208.

[2]Hallock, J. N., Greene, G. C., and Burnham, D. C., "Wake Vortex Research—A Retrospective Look," *Air Traffic Control Quarterly*, Vol. 6, No. 3, 1998, pp. 161–178.

[3]Gurke, T., and Lafferton, H., "The Development of the Wake Vortex Warning System for Frankfurt Airport: Theory and Implementation," *Air Traffic Control Quarterly*, Vol. 5, No. 1, 1997, pp. 3–29.

[4]Le Roux, C., and Corjon, A., "Wake Vortex Advisory System Implementation at Orly Airport for Departing Aircraft," *Air Traffic Control Quarterly*, Vol. 5, No. 1, 1997, pp. 31–48.

[5]Hinton, D. A., "An Aircraft Vortex Spacing System (AVOSS) for Dynamical Wake Vortex Spacing Criteria," *The Characterization and Modification of Wakes from Lifting Vehicles in Fluids*, CP-584, AGARD, 1996, pp. 23.1–23.11.

[6]de Bruin, A., "Wake Vortex Evolution and Encounter (WAVENC)," *AIR and SPACE EUROPE*, Vol. 2, No. 5, 2000, pp. 84–87.

[7]Frech, M., "VORTEX-TDM—A Parameterized Wake Vortex Transport and Decay Model and its Meteorological Input Data Base," DFS Deutsche Flugsicherung, Offenbach, Germany, March 2001.

[8]Frech, M., and Holzäpfel, F., "A Probabilistic Prediction Scheme for Wake Vortex Evolution in a Convective Boundary Layer," *Air Traffic Control Quarterly*, Vol. 10, No. 1, 2002, pp. 23–41.

[9]Greene, G. C., "An Approximate Model of Vortex Decay in the Atmosphere," *Journal of Aircraft*, Vol. 23, No. 7, 1986, pp. 566–573.

[10]Corjon, A., and Poinsot, T., "Vortex Model to Define Safe Aircraft Separation Standards," *Journal of Aircraft*, Vol. 33, No. 3, 1996, pp. 547–553.

[11]Sarpkaya, T., "New Model for Vortex Decay in the Atmosphere," *Journal of Aircraft*, Vol. 37, No. 1, 2000, pp. 53–61.

[12]Sarpkaya, T., Robins, R. E., and Delisi, D. P., "Wake–Vortex Eddy-Dissipation Model Predictions Compared with Observations," *Journal of Aircraft*, Vol. 38, No. 4, 2001, pp. 687–692.

[13]Jackson, W., Yaras, M., Harvey, J., Winckelmans, G., Fournier, G., and Belotserkovsky, A., "Wake Vortex Prediction—An Overview," Transport Canada, Rept. TP 13629E, Montreal, March 2001.

[14]Kantha, L. H., "Empirical Model of Transport and Decay of Wake Vortices Between Parallel Runways," *Journal of Aircraft*, Vol. 33, No. 4, 1996, pp. 752–760.

[15]Mokry, M., "Numerical Simulation of Aircraft Trailing Vortices Interacting with Ambient Shear or Ground," *Journal of Aircraft*, Vol. 38, No. 4, 2001, pp. 636–643.

[16]Holzäpfel, F., Gerz, T., and Baumann, R., "The Turbulent Decay of Trailing Vortex Pairs in Stably Stratified Environments," *Aerospace Science and Technology*, Vol. 5, No. 2, 2001, pp. 95–108.

[17]Proctor, F. H., and Switzer, G. F., "Numerical Simulation of Aircraft Trailing Vortices," 9th Conf. on Aviation, Range and Aerospace Meteorology, Paper 7.12, American Meteorology Society, Orlando, Florida, Sept. 2000, pp. 511–516.

[18]Spalart, P. R., "Airplane Trailing Vortices," *Annual Review of Fluid Mechanics*, Vol. 30, 1998, pp. 107–138.

[19]Holzäpfel, F., Hofbauer, T., Gerz, T., and Schumann, U., "Aircraft Wake Vortex Evolution and Decay in Idealized and Real Environments: Methodologies, Benefits and Limitations," *Advances in LES of Complex Flows*, edited by R. Friedrich and W. Rodi, Vol. 65, Fluid Mechanics and its Applications, Kluwer Academic, Dordrecht, The Netherlands, 2002, pp. 293–309.

[20]Campbell, S. D., Dasey, T. J., Freehart, R. E., Heinrichs, R. M., Matthews, M. P., Perras, G. H., and Rowe, G. S., "Wake Vortex Field Measurement Program at Memphis, TN, Data Guide," Lincoln Lab., Project Rept. NASA/L-2, Massachusetts Inst. of Technology, Cambridge, MA, Jan. 1997.

[21]Hinton, D. A., and Tatnall, C. R., "A Candidate Wake Vortex Strength Definition for Application to the NASA Aircraft Vortex Spacing System (AVOSS)," NASA TM 110343, Sept. 1997, p. 32.

[22]Zierep, J., "Ähnlichkeitsgesetze und Modellregeln der Strömungslehre," Braun, Karlsruhe, Germany, 1982.

[23]Sarpkaya, T., "Decay of Wake Vortices of Large Aircraft," *AIAA Journal*, Vol. 36, No. 9, 1998, pp. 1671–1679.

[24]Holzäpfel, F., Hofbauer, T., Darracq, D., Moet, H., Garnier, F., and Ferreira Gago, C., "Analysis of Wake Vortex Decay Mechanisms in the Atmosphere," *Aerospace Science and Technology* (submitted for publication); also 3rd ONERA–DLR Aerospace Symposium, S3–2, Paris, June 2001, p. 10.

[25]Jeanmart, H., and Winckelmans, G. S., "VLES of Aircraft Wake Vortices in a Turbulent Atmosphere: A Study of Decay," *Advances in LES of Complex Flows*, edited by R. Friedrich and W. Rodi, Vol. 65, Fluid Mechanics and its Applications, Kluwer Academic, Dordrecht, The Netherlands, 2002, pp. 311–326.

[26]Vaughan, J. M., Brown, D. W., Constant, G., Eacock, J. R., and Foord, R., "Structure, Trajectory and Strength of B747 Aircraft Wake Vortices Measured by Laser," *The Characterisation and Modification of Wakes from Lifting Vehicles in Fluids*, CP-584, AGARD, 1996, pp. 10-1–10-10.

[27]Shen, S., Ding, F., Han, J., Lin, Y.-L., Arya, S. P., and Proctor, F. H., "Numerical Modeling Studies of Wake Vortices: Real Case Simulations," AIAA Paper 99-0755, Jan. 1999.

[28]Zinner, T., "Analyse und Modellierung des Verhaltens von Flugzeugwirbelschleppen in der Atmosphäre," Diploma Thesis, Inst. of Atmospheric Physics, DLR, German Aerospace Research Center, Oberpfaffenhofen, Germany, 2001.

[29]Robins, R. E., Delisi, D. P., and Greene, G. C., "Algorithm for Prediction of Trailing Vortex Evolution," *Journal of Aircraft*, Vol. 38, No. 5, 2001, pp. 911–917.

[30]Frech, M., and Zinner, T., "The Concept of Wake Vortex Behaviour Classes and an Analysis of the ICAO Separation Distances," *Journal of Aircraft* (submitted for publication).

[31]Stull, P. R., "An Introduction to Boundary Layer Meteorology," *Atmospheric Sciences Library*, Kluwer Academic, Dordrecht, The Netherlands, 1988, pp. 175–180.

[32]Robins, R. E., and Delisi, D. P., "Further Development of a Wake Vortex Predictor Algorithm and Comparisons to Data," AIAA Paper 99-0757, Jan. 1999.

[33]Dasey, T. J., Cole, R. E., Heinrichs, R. M., Matthews, M. P., and Perras, G. H., "Aircraft Vortex Spacing System (AVOSS) Initial 1997 System Deployment at Dallas/Ft. Worth (DFW) Airport," Lincoln Lab., Project Rept. NASA/L-3, Massachusetts Inst. of Technology, Cambridge, MA, July 1998.

[34]Gerz, T., "Wake Vortex Prediction and Observation: Towards an Operational System," 3rd ONERA–DLR Aerospace Symposium, S1–3, Paris, June 2001, p. 10.